

Electronic Supplementary Information

Journal of Materials Chemistry C

Complete Self-Recovery of Photoluminescence of Photodegraded Cesium Lead Bromide Quantum Dots

Koji Kidokoro, Yoshiki Iso* and Tetsuhiko Isobe*

Department of Applied Chemistry, Faculty of Science and Technology, Keio University,

3-14-1 Hiyoshi, Kohoku-ku, Yokohama 223-8522, Japan

*Corresponding Authors

E-mail address: iso@applc.keio.ac.jp (Y.I.), isobe@applc.keio.ac.jp (T.I.);

Tel: +81 45 566 1558 (Y.I.), +81 45 566 1554 (T.I.); Fax: + 81 45 566 1551

Experimental

Materials

Cs₂CO₃ (99.99%, Mitsuwa Pure Chemical), PbBr₂ (99%, Mitsuwa Pure Chemical), and commercial CsPbBr₃ powder (>98.0%, Tokyo Chemical Industry) were used as received without further purification. 1-Octadecene (>90.0%, Tokyo Chemical Industry), oleic acid (>85.0%, Tokyo Chemical Industry), oleylamine (80–90%, Acros), tert-butanol (>99.0%, Tokyo Chemical Industry), and toluene (99.5%, Kanto Chemical) were dehydrated over molecular sieves (3A 1/8, Wako Pure Chemical Industries) prior to use.

Preparation of CsPbBr₃ QDs

Cs₂CO₃ (2.50 mmol) was added into a mixture of 1-octadecene (40 mL) and oleic acid (2.5 mL). The mixture was dried at 120 °C for 1 h and then heated to 150 °C under Ar gas to yield a cesium oleate solution. The solution was kept at 100 °C. Next, a mixture of 1-octadecene (5 mL) and PbBr₂ (0.376 mmol) was vacuum dried at 120 °C for 1 h and then purged with Ar gas. Oleylamine (1.0 mL) and oleic acid (1.0 mL) were added to the mixture, followed by heating up to 180 °C. PbBr₂ was completely dissolved during the temperature increase. The preheated solution of cesium oleate was rapidly injected into the lead solution, and 10 s later, the resulting CsPbBr₃ QD dispersion was cooled in an

ice-water bath. The QDs were precipitated by the addition of tert-butanol (25 mL) and collected by centrifugation at $\sim 19,000 \times g$ (13,000 rpm using a rotor with a diameter of 10 cm) for 5 min. After vacuum drying for 1 day, the obtained paste-like QD samples were packed in a sample cell (PSH-003, JASCO).

Blue LED irradiation on QDs

The QD sample packed in the cell was irradiated by a flat panel blue LED (TE-4556, Nissin Electronics) equipped with a power supply (LPR-10W, Nissin Electronics) for 72 h (Figure S1). Its luminescent wavelength and irradiance were 468 nm and 48.5 W m^{-2} , respectively. The irradiated sample was stored in the dark at room temperature until measurements. Notably, we observed a slight change in the shape of sample after the irradiation for 72 h and during storage in the dark for 2400 h (Fig. 1a). We suppose that the sticky sample slowly moved into a very narrow gap between the glass window and the PTFE holder, resulting in the change in the shape of sample.

When the QD sample was exposed to ambient air during irradiation and subsequent storage in the dark, the quartz glass window of the cell was eliminated.

Characterization

Thermal images of QDs were captured by a thermography camera (TG167, FLIR). X-ray diffraction (XRD) profiles were obtained with an X-ray diffractometer (Rint-2200, Rigaku) with a Cu K α radiation source and a monochromator. UV-vis absorption spectra were measured using a UV/visible/near-infrared optical absorption spectrometer (V-570, JASCO). The Tauc plot was calculated according to equation (S1) to determine the band gap (E_g) of the QDs.^{S1}

$$(\alpha h\nu)^2 = A(h\nu - E_g), \quad (S1)$$

where α is the absorbance, h is the Planck constant, ν is the frequency, and A is a constant.

PL spectra were measured using a fluorescence spectrometer (FP-8500, JASCO). The obtained spectra were calibrated by using a calibrated detector (SID-844, JASCO). PL decay curves were recorded on a fluorescence lifetime spectrometer (Quantaaurus-Tau C11367, Hamamatsu Photonics) using a Xe flash lamp with a bandpass filter of 340 nm.

Herein, the PL decay curves were fitted with the following triexponential equation:

$$f(t) = A_1 \exp\left(-\frac{t}{\tau_1}\right) + A_2 \exp\left(-\frac{t}{\tau_2}\right) + A_3 \exp\left(-\frac{t}{\tau_3}\right), \quad (S2)$$

where A_1 , A_2 , and A_3 are the amplitudes, and τ_1 , τ_2 , and τ_3 are the PL lifetimes. The average

PL lifetime $\langle\tau\rangle$ was calculated using equation (S3).

$$\langle \tau \rangle = \frac{A_1 \tau_1^2 + A_2 \tau_2^2 + A_3 \tau_3^2}{A_1 \tau_1 + A_2 \tau_2 + A_3 \tau_3} \quad (\text{S3})$$

Absolute PLQY was measured using a fluorescence spectrometer (FP-6500, JASCO) attached with an integrating sphere (ISF-513, JASCO). The QD morphologies were observed by field emission TEM (Tecnai G², FEI). TEM samples were prepared by vacuum drying a drop of QD dispersion in toluene on a carbon-reinforced collodion-coated copper grid (COL-C10, Oken Shoji). Fourier transform infrared (FT-IR) spectra of QDs dispersed in KBr disks were measured on a spectrometer (FT/IR-4200, JASCO).

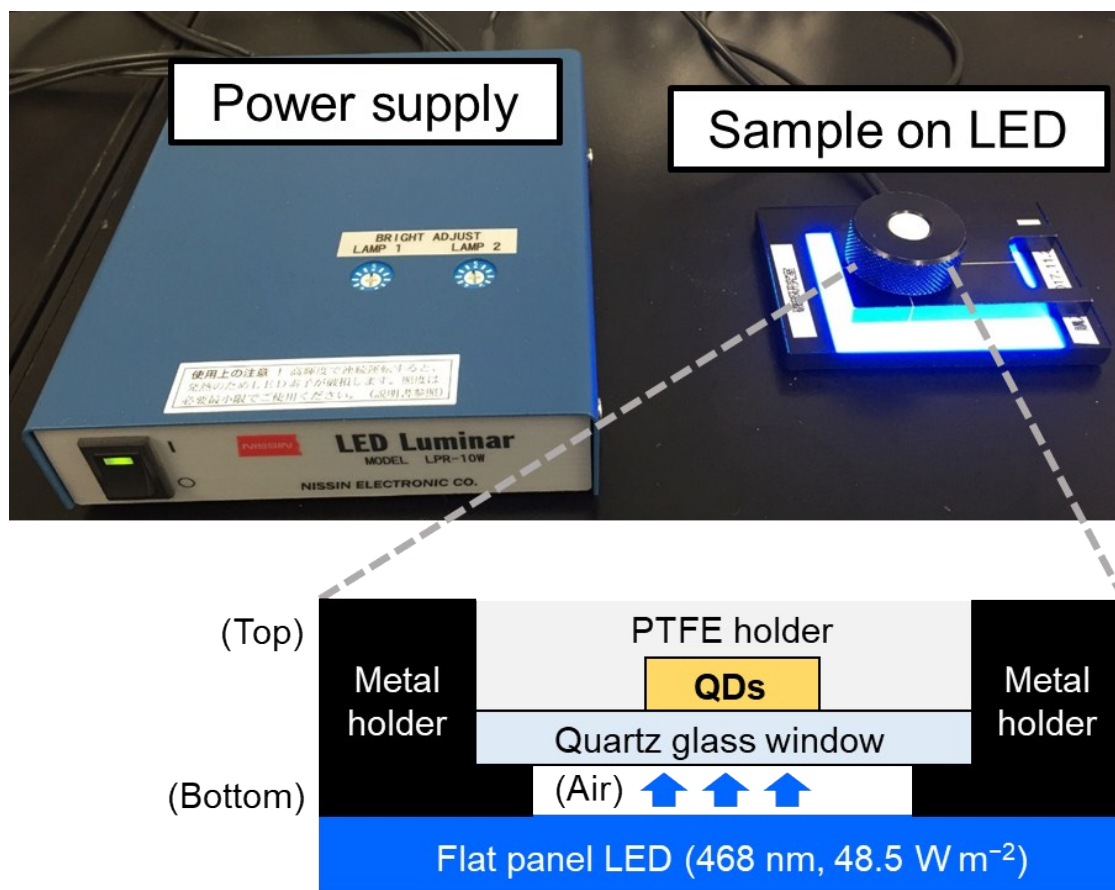


Fig. S1 Photograph and schematic cross-sectional illustration of blue LED irradiation on dried QD samples in the sample cell. The actual experiment was performed in the dark.

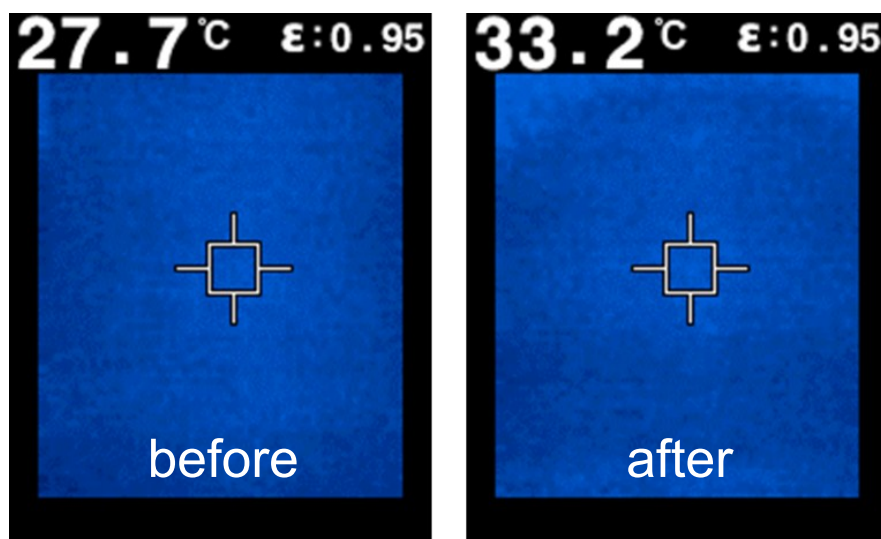


Fig. S2 Thermal images of QDs in the sample cell before and after blue LED irradiation for 72 h. The QD powder is positioned in the center.

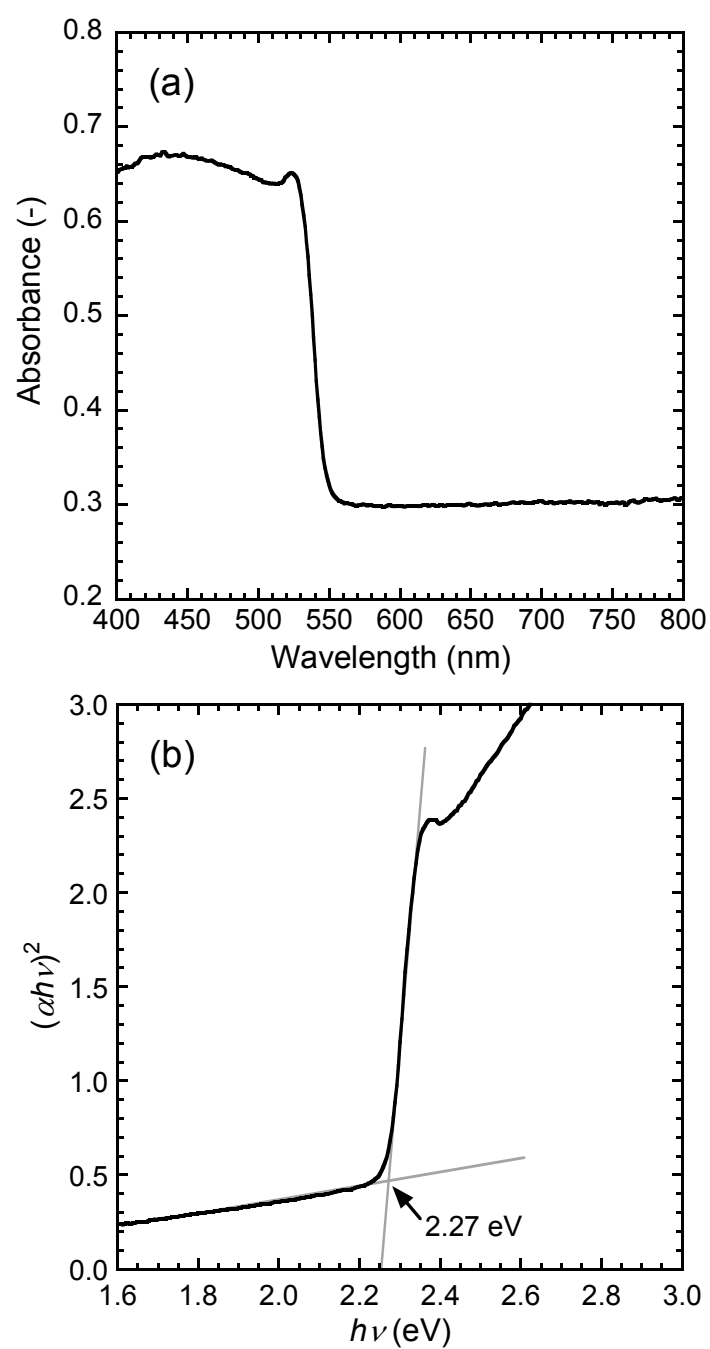


Fig. S3 Estimation of the band gap of the prepared QDs. (a) UV-vis absorption spectrum and (b) corresponding Tauc plot of the as-prepared QD sample.

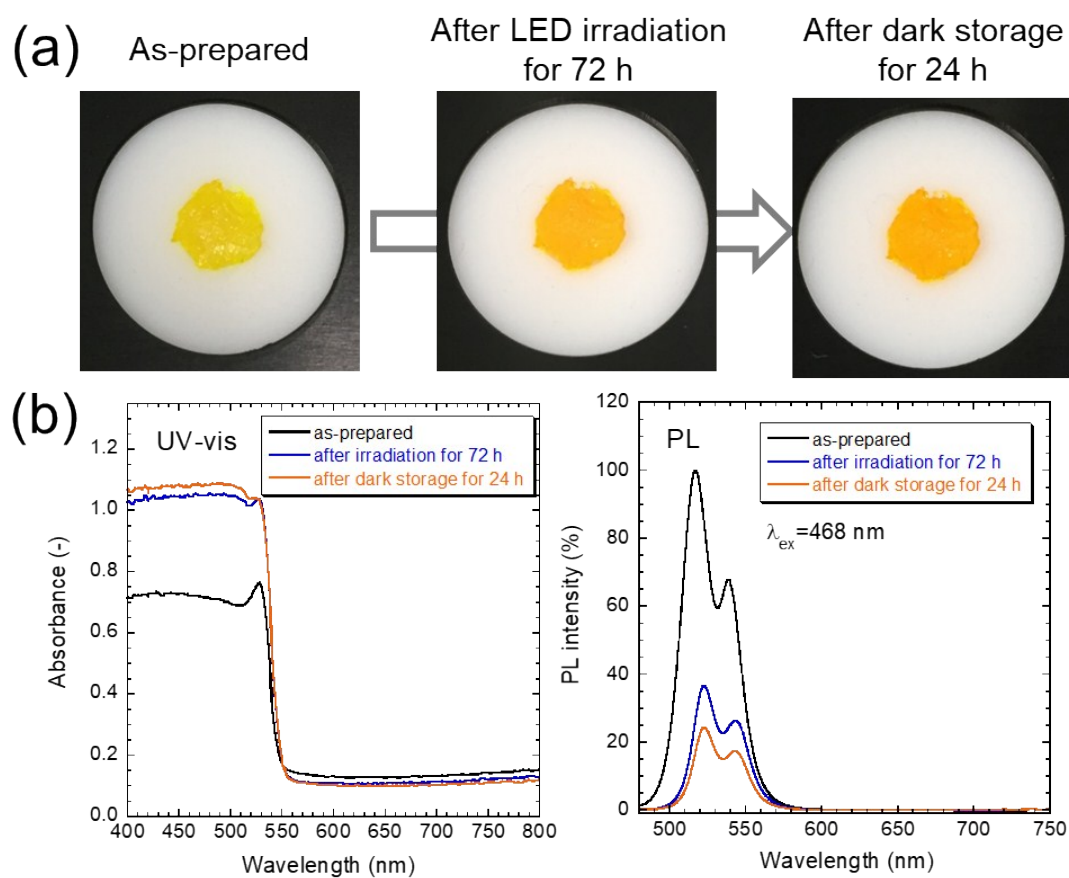


Fig. S4 Results for QDs exposed to ambient air. (a) Changes in the sample color and (b) UV-vis absorption and PL spectra during the experiment.

Table S1 Results of the PL lifetime analysis of the PL decay curves in Figure 2b.

| \square | Average (ns) | PL lifetime (ns) | | | Amplitude (%) | | | χ^2 |
|---------------------------------|----------------------|------------------|----------|----------|---------------|-------|-------|----------|
| \square | $\langle\tau\rangle$ | τ_1 | τ_2 | τ_3 | A_1 | A_2 | A_3 | |
| As-prepared | 103.9 | 7.8 | 36.1 | 225.4 | 78.0 | 18.3 | 3.8 | 1.21 |
| After irradiation for 72 h | 13.2 | 3.5 | 12.9 | 59.4 | 85.8 | 13.1 | 1.1 | 1.08 |
| After dark storage for 24 h | 81.3 | 5.6 | 27.2 | 197.7 | 79.4 | 18.0 | 2.6 | 1.16 |
| After dark storage for 240 h | 105.3 | 5.9 | 31.3 | 223.4 | 78.1 | 18.5 | 3.4 | 1.21 |

Supporting discussion on the asymmetrical PL peak

The observed PL peak from the initial QDs was asymmetrical. Unfortunately, we could not provide a sufficient explanation for the asymmetrical PL peak from the initial sample. Notably, the PL peak of the initial sample redispersed in toluene was symmetrical, as shown in Fig. S5. We assumed that the shape in PL peak would be affected by interaction between QDs. The blue-shift of the PL peak was observed by the redispersion because of a decrease in self-absorption. However, a reason for the disappearance of the shoulder peak was unclear.

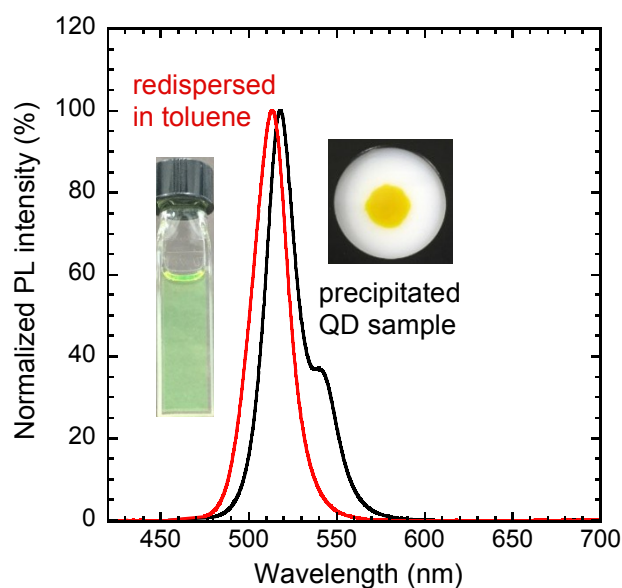


Fig. S5 Normalized PL spectra of paste sample and toluene dispersion for the as-prepared QDs.

Radiative recombination rates for CsPbBr₃ QDs

We also calculated radiative recombination rates corresponding to Fig. 2b. The recombination rates are recombination probabilities per unit; therefore, the radiative and non-radiative recombination rates are given by the equations (S4) and (S5).^{S2}

$$\langle \tau \rangle = (k_r + k_{nr})^{-1} \quad (\text{S4})$$

$$\Phi = k_r(k_r + k_{nr})^{-1} \quad (\text{S5})$$

where $\langle \tau \rangle$ is the average PL lifetime shown in Table S1, k_r and k_{nr} are the radiative and non-radiative recombination rates, respectively, and Φ is the absolute PLQY. The calculated results are summarized in Table S2.

Table S2 Calculated radiative and non-radiative recombination rates.

| | $\langle \tau \rangle$ (ns) | Φ | k_r (s ⁻¹) | k_{nr} (s ⁻¹) |
|------------------------------|-----------------------------|--------|--------------------------|-----------------------------|
| As-prepared | 103.9 | 0.098 | 9.4×10^5 | 8.7×10^6 |
| After irradiation for 72 h | 13.2 | 0.024 | 1.8×10^6 | 7.4×10^7 |
| After dark storage for 24 h | 81.3 | 0.052 | 6.4×10^5 | 1.2×10^7 |
| After dark storage for 240 h | 105.3 | 0.057 | 5.4×10^5 | 9.0×10^6 |

It should be noted that the PLQY of the as-prepared sample was 9.8%, which was lower than >60% for the CsPbBr₃ QD dispersion as reported in our previous work.²⁹ We used precipitated QDs in this work; therefore, energy migration and self-absorption effect should be enhanced, leading to a significant decrease in the PLQY.

Remaining quantum size effect after crystal growth

If the quantum size effect was weakened by the excess crystal growth, a redshift in the UV-vis absorption edge would be observed due to an increase in the band gap.^{S3} The lack of change in the absorption edge and the recovery of the PL properties both indicate that the quantum size effect was maintained after crystal growth. Therefore, the grown QDs might have a nanosheet-like morphology with a thickness small enough to maintain the quantum size effect. This explanation may be supported by the elongated particles observed in the 72-h irradiated sample (Fig. 3). Instead of the expected nanosheets, apparent rod-like particles were observed. The thickness of the rod-like particles was less than 10 nm, which revealed that the crystals did not grow along the thickness direction. The XRD profiles exhibited changes in the relative peak intensities (Fig. S6). Herein, the peak of the (200) plane of cubic CsPbBr₃ only became stronger, indicating anisotropic crystal growth. We speculated that the QDs in contact with the glass window of the sample cell grew parallel to the window during the LED irradiation. It should be noted that other crystal phases in addition to cubic CsPbBr₃ were not observed in the XRD analysis even after the subsequent dark storage. Thus, the photodegradation and subsequent self-recovery in the dark were not caused by changes in the particle morphology and structure.

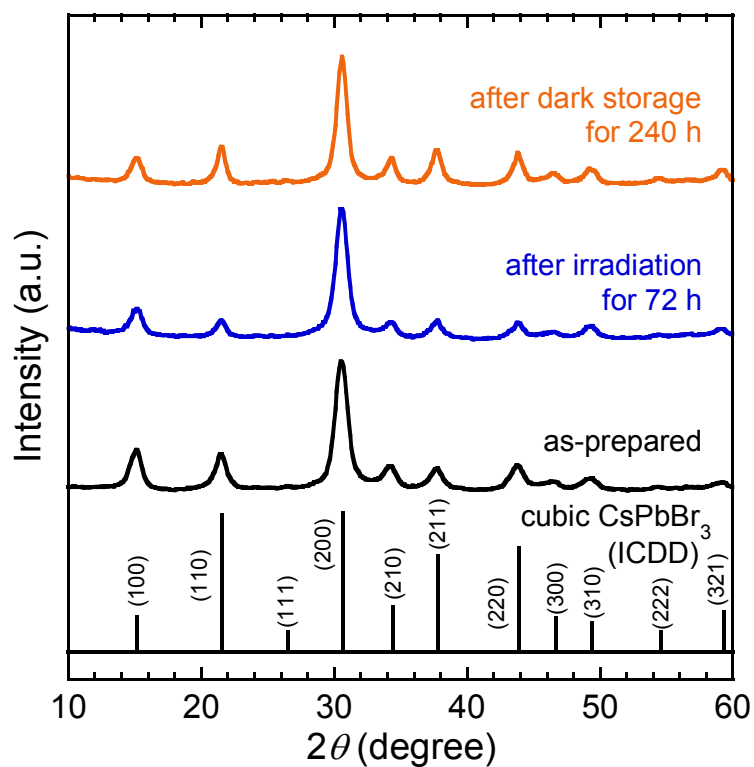


Fig. S6 Influence of irradiation on the crystal structure of QDs. XRD profiles of QDs before and after blue LED irradiation for 72 h and after the subsequent storage in the dark for 240 h. ICDD card data of cubic and monoclinic CsPbBr₃ (Nos. 00-054-0752 and 00-054-0751, respectively) are also shown.

Results using commercial CsPbBr₃ without surface ligands

To verify the influence of the surface ligands, we performed the same experiment using commercial CsPbBr₃ without surface ligands. The purchased CsPbBr₃ powder was purged with an inert gas to avoid surface oxidation by ambient air. As shown in the FT-IR spectrum in Fig. S7a, the absence of the peaks assigned to the CH stretching modes { $\nu(\text{CH})$ } derived from the surface ligands was confirmed. Consequently, changes in the UV-vis absorption and sample color were not observed after irradiation of the commercial sample (Fig. S7b and c), supporting the proposal that the blackening of the QDs is due to a change in the surface state of the surface ligands.

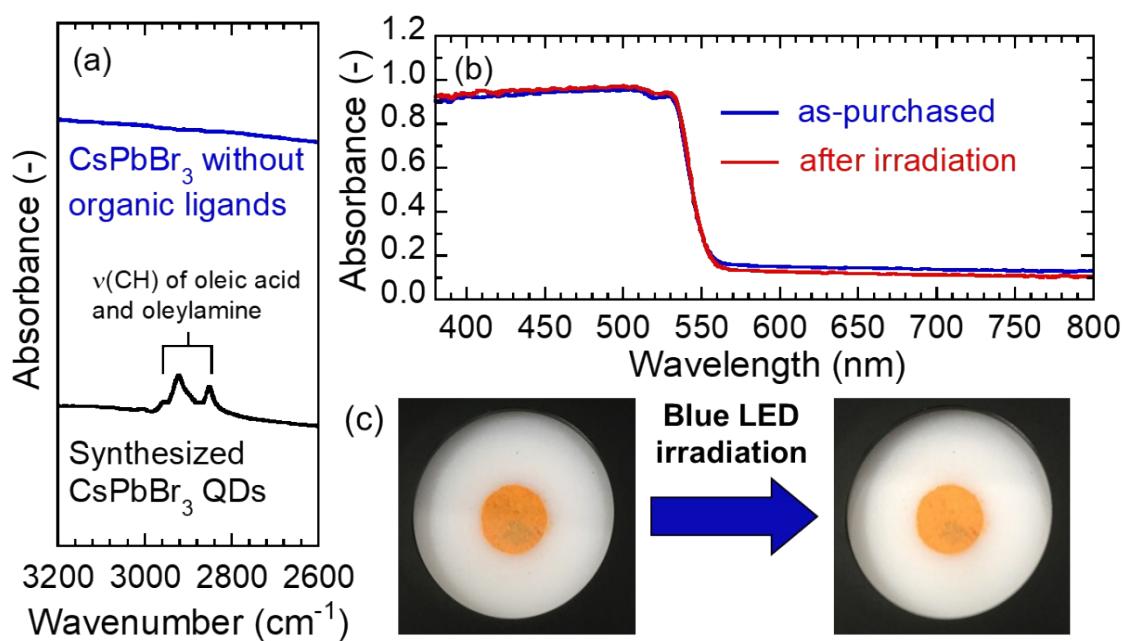


Fig. S7 Results using commercial CsPbBr₃. (a) FT-IR spectra of commercial CsPbBr₃ and the synthesized CsPbBr₃ QDs. (b) UV-vis spectra and (c) photographs of the commercial sample before and after blue LED irradiation.

References

- S1. J. Tauc and A. J. Menth, *J. Non-Cryst. Solids*, 1972, **8–10**, 569–585.
- S2. E. Nakazawa, in *Phosphor Handbook*, ed. S. Shionoya and W. M. Yen, CRC Press, Boca Raton, 1st ed., 1999, Chapter 2—Section 7, p. 86.
- S3. M. C. Brennan, J. E. Herr, T. S. Nguyen-Beck, J. Zinna, S. Draguta, S. Rouvimov, J. Parkhill and M. Kuno, *J. Am. Chem. Soc.*, 2017, **139**, 12201–12208.